Ultrafast X-Ray Spectroscopy of Conical Intersections

Simon P. Neville,[1,2] Majed Chergui,[2] Albert Stolow,[1,3,4] and Michael S. Schuurman[1,3]

[1]*Department of Chemistry and Biomolecular Sciences, University of Ottawa,*
10 Marie Curie, Ottawa, Ontario K1N 6N5, Canada
[2]*Ecole Polytechnique Fédédrale de Lausanne, Laboratoire de Spectroscopie Ultrarapide and Lausanne Centre*
for Ultrafast Science (LACUS), Faculté des Sciences de Base, ISIC, Lausanne CH-1015, Switzerland
[3]*National Research Council of Canada, 100 Sussex Drive, Ottawa, Ontario K1A 0R6, Canada*
[4]*Department of Physics, University of Ottawa, 150 Louis Pasteur, Ottawa, Ontario K1N 6N5, Canada*

Ongoing developments in ultrafast x-ray sources offer powerful new means of probing the complex nonadiabatically coupled structural and electronic dynamics of photoexcited molecules. These non-Born-Oppenheimer effects are governed by general electronic degeneracies termed conical intersections, which play a key role, analogous to that of a transition state, in the electronic-nuclear dynamics of excited molecules. Using high-level *ab initio* quantum dynamics simulations, we studied time-resolved x-ray absorption (TRXAS) and photoelectron spectroscopy (TRXPS) of the prototypical unsaturated organic chromophore, ethylene, following excitation to its $S_2(\pi\pi^*)$ state. The TRXAS, in particular, is highly sensitive to all aspects of the ensuing dynamics. These x-ray spectroscopies provide a clear signature of the wave packet dynamics near conical intersections, related to charge localization effects driven by the nuclear dynamics. Given the ubiquity of charge localization in excited state dynamics, we believe that ultrafast x-ray spectroscopies offer a unique and powerful route to the direct observation of dynamics around conical intersections.

In excited states of polyatomic molecules, conical intersections (CIs) play a central role, analogous to transition states in ground state dynamics. As with transition states, the spatial range of the conical intersection dynamics is somewhat extended beyond the CI (a point of electronic degeneracy) itself. In the following, therefore we use the term conical intersection to refer to this spatial region. Despite their widespread use in rationalizing ultrafast electronic-nuclear dynamics [1], the unambiguous experimental observation of CIs remains elusive. Here we investigate the use of ultrafast x-ray spectroscopies to directly observe dynamics at CIs. This is motivated by recent technological advances which result in the availability of powerful ultrafast light sources in the x-ray regime. The use of x rays is appealing, because they offer an atom-specific probe of electronic and structural dynamics. While most x-ray spectroscopic studies of molecular dynamics were initially performed in the hard x-ray range [2–4], studies have also recently appeared in the soft x-ray range [5], in particular, using tabletop sources [6,7].

There are a growing number of theoretical proposals for the use of x-ray spectroscopies as probes of ultrafast non-adiabatic dynamics in photoexcited molecules [8–13]. Of these, only two techniques, namely, time-resolved x-ray absorption spectroscopy (TRXAS) and time-resolved x-ray photoelectron spectroscopy (TRXPS), have demonstrated experimental feasibility and are therefore the focus of the present study. We recently showed that the pre-edge region of the x-ray absorption spectrum offers a uniquely sensitive probe of dynamics in the most fundamental unsaturated hydrocarbon, the planar C_2H_4 molecule ethylene [9]. Specifically, the computed time-resolved carbon K-edge absorption spectrum contained clear signatures of the excited state wave packet dynamics [9,10]. Here we apply this approach to the spectroscopy of CIs, an important goal of ultrafast molecular sciences. In our previous work on valence shell time-resolved photoelectron spectroscopy (TRPES), we showed that the outgoing photoelectron is a particularly insightful probe of nonadiabatic dynamics in molecules [14–16]. Therefore, we also simulate here the inner shell TRXPS for the same photoinitiated process. We believe that this comparison will help design the next generation of x-ray spectroscopy experiments which are just emerging [6,7,17].

Via our simulations, we have uncovered a key advantage of ultrafast x-ray spectroscopy: that charge localization effects in photoexcited ethylene lead to large (few eV) splittings in the excited state pre-edge x-ray absorption spectrum. This, in turn, offers a unique and acute sensitivity to wave packet dynamics at a CI. This observation has far-reaching consequences, given the commonality of charge localization in excited state molecular dynamics and biological processes such as proton and electron transfer.

Our methods for calculating TRXAS were described in detail elsewhere [9]. Likewise, our simulations of TRXPS

are directly analogous to previously described methodologies for computing valence shell electron (UV) TRPES [18]. Accordingly, we give only a brief summary of the computational methodology here, with further details offered in Supplemental Material [19]. The *ab initio* multiple spawning (AIMS) method [27] was used to describe the time evolution of the excited state wave packet. In the AIMS method, the molecular wave function is expanded in a set of adiabatic electronic functions, $\{|I(\mathbf{r};\mathbf{R})\rangle\}$, and frozen Gaussian nuclear basis functions, $\{|g_j^{(I)}(\mathbf{R},t)\rangle\}$, of the Heller form:

$$|\Psi(\mathbf{R},\mathbf{r},t)\rangle = \sum_{I=1}^{n_s}\sum_{j=1}^{N_I} C_j^{(I)}(t)|g_j^{(I)}(\mathbf{R},t)\rangle|I(\mathbf{r};\mathbf{R})\rangle. \quad (1)$$

The positions and momenta of the Gaussian basis functions evolve according to the classical equations of motion, and the expansion coefficients are evolved variationally via the solution of the time-dependent nuclear Schrödinger equation. The AIMS equations of motion were solved on the fly using the results of electronic structure calculations performed at the multireference first-order configuration interaction (MR FOCI) level of the theory. The details of these calculations are given in Supplemental Material [19].

In Fig. 1, we schematically show the relevant electronic states as a function of the torsional angle between the two planes defined by each of the CH_2 groups in the molecule. Following vertical excitation of the $S_2(\pi\pi^*)$ state, the wave packet is localized at the structural and electronic character labeled "A." In line with previous studies [28–31], a rapid evolution of the initially excited S_2 state occurs by a large amplitude twisting motion about the C—C bond, leading to
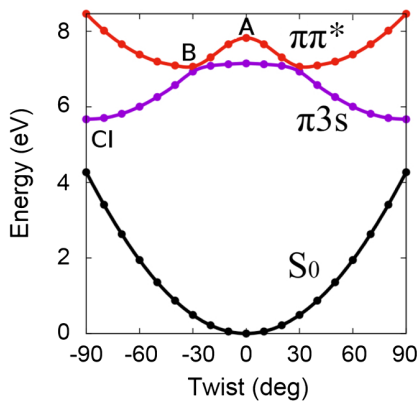

FIG. 1. Relevant electronic states in ethylene as a function of the torsional angle about the C—C bond. The dynamics simulation initializes the wave packet at the FC geometry on the $S_2(\pi\pi^*)$ state (point "A"). The crossing between the initial $\pi\pi^*$ state and the $\pi3s$ state is denoted "B." The important conical intersection with the ground state is labeled "CI" and is the dynamical gateway ("transition state") for the excited state.

a change in the electronic character. The S_1 state is transiently populated and has an electronic structure characterized by both valence $\pi\pi^*$ and Rydberg $\pi3s$ character (point "B"). The total excited state lifetime was determined to be ~95 fs. Internal conversion to the S_0 ground state was found to occur via a so-called twisted-pyramidalized (Tw-Py) CI seam (point "CI"). This CI structure involves a $90°$ twist about the C=C double bond, combined with pyramidalization at one of the C atoms.

We first examine the ability of TRXAS to probe this coupled electronic and nuclear dynamics. The pre-edge part of the TRXAS, $\sigma(E,t)$, was calculated as an incoherent sum over the transient spectra at the centers of the Gaussian basis functions:

$$\sigma(E,t) = \sum_{I=1}^{n_s}\sum_{j=1}^{N_I} |C_j^{(I)}(t)|^2 \sigma_I[E;\bar{\mathbf{R}}_j^{(I)}(t)]. \quad (2)$$

Here, $\sigma_I[E;\mathbf{R}_j^{(I)}(t)]$ denotes the x-ray absorption spectrum (XAS) for the Ith electronic state calculated at the center $\bar{\mathbf{R}}_j^{(I)}(t)$ of the Gaussian basis function $g_j^{(I)}(t)$. The XAS were calculated using the second-order algebraic diagrammatic construction (ADC) method within the core-valence separation approximation [32] and the $6-311++G^{**}$ basis.

In Fig. 2(a), we show the time evolution of the C K-edge x-ray absorption near edge fine structure spectrum following excitation to the $S_2(\pi\pi^*)$ state, while Fig. 2(b) focuses on the pre-edge region only (< 295 eV). The postedge NEXAFS region reflects structural dynamics in the excited molecule and will be discussed in a future publication. Feature A at $t=0$ and 277 eV is assigned to the excitation of the initially prepared $\pi\pi^*$ state to the $1s\pi^*$ core-excited state [9]. The sweep of this feature to higher energies is a result of rapid twisting about the C—C bond, lowering the energy of the $\pi\pi^*$ state. Feature B, beginning at around 281 eV and 10 fs, corresponds to two components of the wave packet: (i) the portion in the transiently populated $\pi3s$ state which transitions to the $1s3s$ and (ii) the component passing through the Tw-Py CI seam. The feature labeled CI, centered around 286 eV, begins to develop intensity at around ~10 fs. It is also assigned to core excitation from the $\pi\pi^*$ state. Significantly, the CI feature originates only from those components of the wave packet in the $\pi\pi^*$ state that are in close proximity to the Tw-Py CI seam. In other words, the calculated TRXAS reveals a clear and direct signature of the arrival of the excited state wave packet at the CI. Finally, the broad, intense set of peaks appearing at times $t \gtrsim 50$ fs in Fig. 2(a) corresponds to the vibrationally hot ground electronic state which appears following passage through the CI.

The most remarkable feature of the calculated TRXAS is that it clearly encodes the arrival of the wave packet at the Tw-Py CI. Figures S1–S5 in Supplemental Material [19]
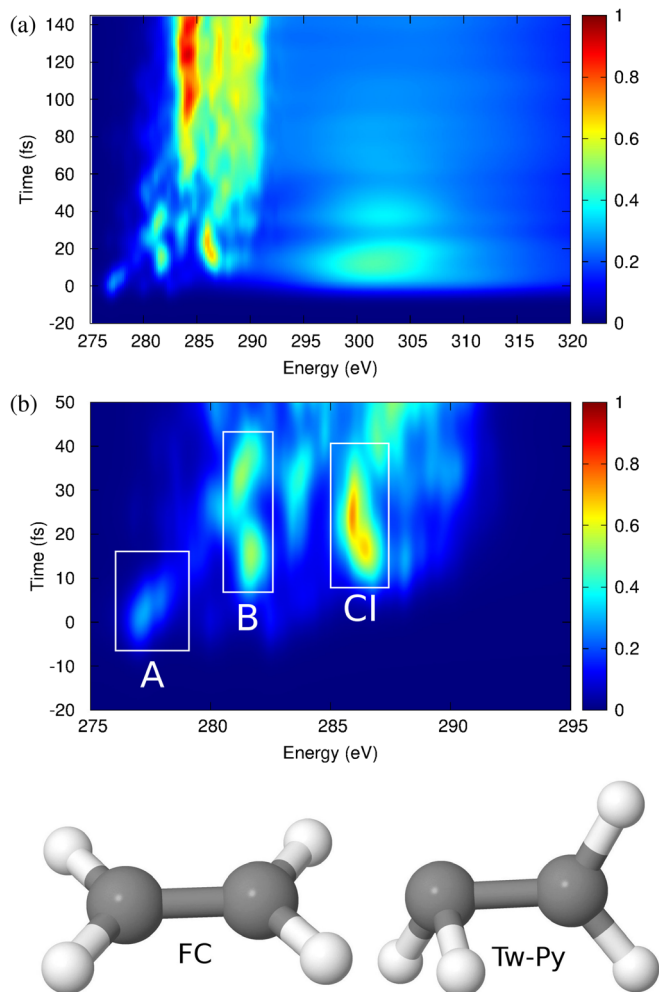
FIG. 2. The TRXAS spectrum calculated from AIMS simulations of ethylene excited to its $\pi\pi^*$ state. (a) The full spectrum showing both the pre-edge and postedge continuum absorption. (b) The pre-edge part of the spectrum at short times and the relevant peak assignments. The features labeled A, B, and CI are directly related to the associated dynamical features shown in Fig. 1. The FC (A) and Tw-Py intersection (CI) geometries are shown below. The color map represents the relative probability of absorption.

show the XAS calculated at two relevant geometries for the states involved and are a convenient reference for the following discussion. Importantly, we find that, at geometries close to the Tw-Py CI geometry, a remarkable splitting appears in the higher-energy peak for the $\pi\pi^*$ state (corresponding to the S_1 state at this geometry) pre-edge XAS. At the initial Franck-Condon (FC) point labeled A, the $\pi\pi^*$ state pre-edge XAS is dominated by a single transition corresponding to the excitation of a $1s$ core electron into the hole in the singly occupied π orbital. At the FC point, the molecule possesses D_{2h} symmetry, meaning that the two $1s$ orbitals are delocalized across the two indistinguishable C atoms, and only excitation from the a_g $1s$ orbital into the π orbital is dipole allowed. That is,

only one $1s \rightarrow \pi$ transition is dipole allowed at this point. Upon pyramidalization at one of the C atoms, the symmetry is lowered and the two C atoms now become distinguishable. The consequences of this are twofold: (i) The $1s$ orbitals now become localized about the C atoms; (ii) excitation from both of these $1s$ orbitals into the π orbital hole now becomes dipole allowed. Accordingly, two distinguishable $1s \rightarrow \pi$ transitions now appear in the XAS. Importantly, as we discuss below, the splitting between the two transition energies is quite large, $\sim$4.5 eV, due to the significant difference in the local valence electronic structure that develops around each of the C atoms. In other words, the charge separation driven by the nonadiabatic dynamics is probed in an atom-specific manner by XAS from each of the now localized, distinguishable $1s$ orbitals.

Since the nonadiabatic AIMS dynamics simulations which underlie the TRXAS spectrum are identical to those used in the calculated TRXPS spectrum, the relative sensitivities of these two techniques to dynamics at CIs can be compared. In Fig. 3, we show the AIMS simulation of the TRXPS spectrum for these same molecular dynamics. At time $t = 0$, the TRXPS is dominated by a single peak corresponding to ionization of the initially prepared $\pi\pi^*$ state in the FC region. Interestingly, the fingerprints of the dynamical evolution are somewhat less clear than in the TRXAS.

Figures S6–S10 show the static x-ray photoelectron spectra (at a photon energy of 320 eV) at two key geometries (FC A and Tw-Py CI) for ionization from the relevant electronic states. At early time delays, feature B in the 314–318 eV region in Fig. 3 shows ionization from $\pi 3s$ but is overlapped with allowed ionization channels from the $\pi\pi^*$ FC geometry A, as well as ionization from S_1 at the Tw-Py CI. Regarding the latter, the splitting of the two inequivalent C $1s$ centers at the Tw-Py CI manifests itself in the splitting between the group of two peaks centered at 299 eV and the group of two peaks at 306 eV in Fig. S9. However, in the wave packet simulation, these peaks overlap somewhat with the bright peak near 304 eV corresponding to ionization of the initially prepared $\pi\pi^*$, obscuring somewhat the signature of the CI.

Confirmation of the origin of this large splitting of the core-excitation energies close to the Tw-Py CI comes from consideration of a one-particle, one-hole ($1p1h$) excitation operator $\hat{C}_{\nu c} = \hat{c}_\nu^\dagger \hat{c}_c$ applied to the correlated ground electronic state $|\Psi_0\rangle$ to yield the singly core-excited configuration $|\Psi_{\nu c}\rangle = \hat{C}_{\nu c}|\Psi_0\rangle$, where c indexes a core orbital and ν a virtual valence orbital. Applying the second-order perturbation theory, the core-excitation energy $\Delta E_{\nu c}$ obtained using the unperturbed $1p1h$ configuration $|\Psi_{\nu c}\rangle$ can be written as [33,34]

$$\Delta E_{\nu c} = [\epsilon_\nu - \epsilon_c] + [2\langle c\nu|\nu c\rangle - \langle c\nu|c\nu\rangle] + \Delta E_{\nu c}^{(2)}. \quad (3)$$

Here, ϵ_p denotes the energy of the pth canonical Hartree-Fock orbital. At the Tw-Py CI geometry, the splitting of the two pre-edge $\pi\pi^*$ state peaks is accounted for almost
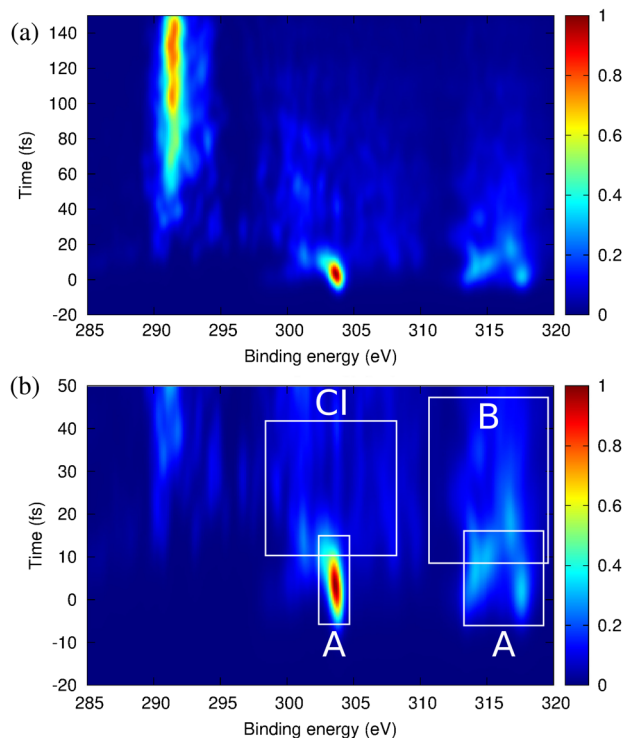
FIG. 3. TRXPS calculated using the results of AIMS simulations of ethylene excited to the $\pi\pi^*$ state. A probe photon energy of 320 eV is assumed. (a) The spectrum for all simulation times. (b) The spectrum focused on short times. The features labeled A, B, and CI are related to the dynamical features shown in Fig. 1. The color map represents the relative probability of ionization.

entirely by the zeroth-order term $[\epsilon_\nu - \epsilon_c]$. Importantly, the splitting of the two peaks is a consequence of the splitting of the corresponding $1s$ orbital energies due to the distinguishability of the two C atoms which occurs uniquely at the CI.

The physical picture emerging from this analysis is that the splitting of the C $1s$ peaks is correlated with the onset of charge separation across the C—C bond (the so-called sudden polarization effect) [35], which occurs uniquely at the CI. To confirm this, we use the following metric for charge separation $\Theta(t)$ across the C—C bond derived from the AIMS simulation:

$$\Theta(t) = \sum_{I=1}^{n_s} \sum_{j=1}^{N_I} |C_j^{(I)}(t)|^2 |\langle g_j^{(I)}(t)|\langle I|\boldsymbol{\mu}\cdot\boldsymbol{\nu}_{CC}|I\rangle|g_j^{(I)}(t)\rangle|. \quad (4)$$

Here, $\boldsymbol{\mu}$ denotes the molecular dipole operator and $\boldsymbol{\nu}_{CC}$ the unit vector coincident with the C—C bond. The nuclear part of the integral $\langle g_j^{(I)}|\langle I|\boldsymbol{\mu}\cdot\boldsymbol{\nu}_{CC}|I\rangle|g_j^{(I)}\rangle$ is evaluated analytically, while the electronic part is evaluated using a first-order saddle point approximation. The short-time evolution of $\Theta(t)$ is shown in Fig. 4. It is clear that charge separation across the C—C bond occurs rapidly, with a local maximum value of Θ being attained at around 10 fs. This
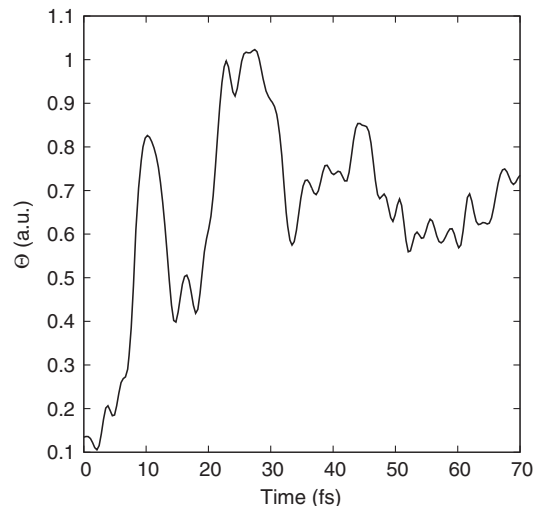

FIG. 4. Time evolution of the charge transfer metric Θ calculated using the results of AIMS simulations of ethylene excited to the $\pi\pi^*$ state. The large, transient charge separations occurs when the wave packet encounters the Tw-Py CI and is responsible for the distinguishability of the two C atoms at the CI.

correlates with the appearance and initial growth in intensity of the peak centered at 286 eV in the calculated TRXAS (Fig. 2). The onset of charge separation at the CI leads to the splitting of the peaks in $\pi\pi^*$ state pre-edge XAS. The magnitude of this splitting is a consequence of the separation of the $1s$ orbital energies, as a result of the transient charge separation across the C—C bond that occurs uniquely at the CI. We expect this to be a general feature of dynamics at CIs in molecules containing C═C double bonds. Such molecules play central roles in photochemistry, photobiology, and material science.

On the basis of these AIMS simulations, we are emboldened to draw some conclusions. First, employing core electrons to probe valence electron density via ultrafast x-ray spectroscopy results in an exquisitely sensitive measure of complex, dynamic electronic structures. While both TRXAS and TRXPS encode the nonadiabatic dynamics, the overlapping continua in the TRXPS may tend to obscure the CI dynamics. In contrast, TRXAS has fewer dipole-allowed transitions, leading to a direct mapping of absorption peaks to specific dynamical features. We conclude that ultrafast x-ray spectroscopy is a particularly powerful probe of dynamics at conical intersections. The commonality of charge separation dynamics (e.g., proton or electron transfer) in molecular, biological and material processes suggests that TRXAS and TRXPS will have broad applicability, leading to a "transition state spectroscopy" of the excited state. Work is now in progress, within our group and elsewhere, to implement these findings experimentally.

---

[1] W. Domcke, D. R. Yarkony, and H. Köppel, *Conical Intersections: Electronic Structure, Dynamics and Spectroscopy* (World Scientific, Singapore, 2004), Vol. 15, Chap. 1, p. 3.

[2] C. Bressler *et al.*, Science **323**, 489 (2009).

[3] H. T. Lemke *et al.*, J. Phys. Chem. A **117**, 735 (2013).

[4] W. Zhang *et al.*, Nature (London) **509**, 345 (2014).

[5] N. Huse, H. Cho, K. Hong, L. Jamula, F. M. F. de Groot, T. K. Kim, J. K. McCusker, and R. W. Schoenlein, J. Phys. Chem. Lett. **2**, 880 (2011).

[6] A. R. Attar, A. Bhattacherjee, C. D. Pemmaraju, K. Schnorr, K. D. Closser, D. Prendergast, and S. R. Leone, Science **356**, 54 (2017).

[7] Y. Pertot *et al.*, Science (to be published).

[8] G. Capano, C. J. Milne, M. Chergui, U. Rothlisberger, I. Tavernelli, and T. J. Penfold, J. Phys. B **48**, 214001 (2015).

[9] S. P. Neville, V. Averbukh, S. Patchkovskii, M. Ruberti, R. Yun, M. Chergui, A. Stolow, and M. S. Schuurman, Faraday Discuss. **194**, 117 (2016).

[10] S. P. Neville, V. Averbukh, M. Ruberti, R. Yun, S. Patchkovskii, M. Chergui, A. Stolow, and M. S. Schuurman, J. Chem. Phys. **145**, 144307 (2016).

[11] M. Kowalewski, K. Bennett, K. E. Dorfman, and S. Mukamel, Phys. Rev. Lett. **115**, 193003 (2015).

[12] W. Hua, S. Oesterling, J. D. Briggs, Y. Zhang, H. Ando, R. de Vivie-Riedle, B. P. Fingerhut, and S. Mukamel, Struct. Dyn. **3**, 023601 (2016).

[13] M. Kowalewski, B. P. Fingerhut, K. E. Dorfman, K. Bennett, and S. Mukamel, Chem. Rev. **117**, 12165 (2017).

[14] A. Stolow, A. E. Bragg, and D. M. Neumark, Chem. Rev. **104**, 1719 (2004).

[15] O. Schalk, A. E. Boguslavskiy, A. Stolow, and M. S. Schuurman, J. Am. Chem. Soc. **133**, 16451 (2011).

[16] S. P. Neville, Y. Wang, A. E. Boguslavskiy, A. Stolow, and M. S. Schuurman, J. Chem. Phys. **144**, 014305 (2016).

[17] A. Johnson, L. Miseikis, D. Wood, D. Austin, C. Brahms, S. Jarosch, C. Strueber, P. Ye, and J. Marangos, Struct. Dyn. **3**, 062603 (2016).

[18] H. R. Hudock, B. G. Levine, A. L. Thompson, H. Satzger, D. Townsend, N. Gador, S. Ullrich, A. Stolow, and T. J. Martínez, J. Phys. Chem. A **111**, 8500 (2007).

[19] See Supplemental Material at http://link.aps.org/supplemental/10.1103/PhysRevLett.120.243001 for details on the wave packet simulations, as well as additional x-ray absorption and photoelectron spectra employed for the interpretation of the time-resolved data. This material includes Refs. [20–26].

[20] B. T. Pickup, Chem. Phys. **19**, 193 (1977).

[21] M. Spanner, S. Patchkovskii, C. Zhou, S. Matsika, M. Kotur, and T. C. Weinacht, Phys. Rev. A **86**, 053406 (2012).

[22] B. O. Roos, M. P. Fülscher, P. A. Malmqvist, M. Merchán, and L. Serrano-Andrés, *Quantum Mechanical Electronic Structure Calculations with Chemical Accuracy* (Kluwer Academic, Dordrecht, 1995), p. 357.

[23] H. Lischka *et al.*, Columbus, an *ab initio* electronic structure program, release 7.0, 2012.

[24] J. F. Stanton *et al.*, Cfour, coupled-cluster techniques for computational chemistry, a quantum-chemical program package; see http://www.cfour.de.

[25] H. Tao, T. K. Allison, T. W. Wright, A. M. Stooke, C. Khurmi, J. van Tilborg, Y. Liu, R. W. Falcone, A. Belkacem, and T. J. Martínez, J. Chem. Phys. **134**, 244306 (2011).

[26] H. Tao, B. G. Levine, and T. J. Martínez, J. Phys. Chem. A **113**, 13656 (2009).

[27] M. Ben-Nun and T. J. Martínez, Adv. Chem. Phys. **121**, 439 (2002).

[28] T. Mori, W. J. Glover, M. S. Schuurman, and T. J. Martínez, J. Phys. Chem. A **116**, 2808 (2012).

[29] E. G. Champenois, N. H. Shivaram, T. W. Wright, C. S. Yang, A. Belkacem, and J. P. Cryan, J. Chem. Phys. **144**, 014303 (2016).

[30] T. Kobayashi, T. Horio, and T. Suzuki, J. Phys. Chem. A **119**, 9518 (2015).

[31] T. K. Allison *et al.*, J. Chem. Phys. **136**, 124317 (2012).

[32] J. Wenzel, A. Holzer, M. Wormit, and A. Dreuw, J. Chem. Phys. **142**, 214104 (2015).

[33] J. Schirmer, Phys. Rev. A **26**, 2395 (1982).

[34] J. Schirmer, M. Braunstein, M. T. Lee, and V. McKoy, *VUV and Soft X-Ray Photoionization* (Plenum, New York, 1996), Chap. 4, p. 105.

[35] B. R. Brooks and H. F. Schaefer, J. Am. Chem. Soc. **101**, 307 (1979).